Detection of PMSM Inter-Turn Short-Circuit Based on a Fault-Related Disturbance Observer

Ilioudis C. Vasilios

Department of Industrial Engineering and Management, Faculty of Engineering, International Hellenic University (IHU), Thessaloniki, Greece.

Email: Ilioudis@auth.gr

***Abstract* - This work is focused on inter-turn short-circuit located at a stator phase winding of the permanent magnet synchronous machine (PMSM). Considering the PMSM behavior under fault, the mathematical model has been developed aiming to detect accurately the stator inter-turn fault in dq synchronous frame. A simple method is proposed able to diagnose the stator windings damage in an initial stage based on a sliding mode observer (SMO) for stator flux. After observer convergence, the derived equivalent control signals are used to estimate the caused voltage disturbance. In evaluating the performance of the inter-turn fault detection algorithm, the magnetic saturation is taken into account in presence of faulty conditions. Since the produced flux distortion is strongly related to the nature and extent of the phase fault, the analysis of the associated waveforms could appeal a precise fault description. Simulation results illustrate the effectiveness of the proposed fault diagnosis and prognosis method in determining an inter-turn phase fault during steady and transient state operation.**

Keywords - Phase Fault Detection, PMSM Fault Analysis, Phase Inter-Turn Short-Circuit, Voltage Disturbance Observer.

I. INTRODUCTION

Nowadays Permanent Magnet Synchronous Machine (PMSM) is extensively used in a plethora of industrial applications. Due to their high power density and high efficiency, the PMSM applications may extend in a wide range, spanning from automotive engineering to robotics, electric traction and renewal energy conversion systems (e.g. wind power turbines) [1], [2]. In general, PMSM speed and position can be effectively controlled adjusting the stator current through advanced control methods, such as field oriented (FOC) or direct torque control (DTC). A noteworthy advantage of PMSMs is that their rotor field is provided by the permanent magnets instead of additional excitation windings. In the absence of an extra field circuit attached on the rotor, the electrical circuitry failures (e.g. phase inter-turn short circuits) are limited and can be isolated in the stator part of PMSM. The deterioration of the windings insulation is the main reason of stator circuitry failures. Excessive temperatures, electrical or mechanical stress, manufacturing defects and environmental issues are among the main causes of the windings insulation impairment resulting to faulty or damaged PMSM. Insulation damage might lead to a short circuit between different segments of AC machine [3]-[5].

The short circuits are the most frequent detected faults occurring in stator winding turns of AC machines, while the inter turn short circuits are the more common faults associated with PMSM [6]. Depending on the machine parts involved, short circuit failures of stator winding can be typically classified into three types: phase-to-ground, phase-to-phase and turn-to-turn of the same phase. Even though the turn-to-urn fault is typically limited only in a small portion of the phase winding associated, this kind of short circuit affects dramatically the PMSM operation causing impaired damages. As long as the machine is still rotating, excessive stator voltages are applied during frequent start and stop states [3]. Under these conditions, the induced current in the faulted turns may exceed the rated one. Therefore methods for early fault detection and machine diagnosis are very important to prevent serious damage and avoid unsafe operation of PMSM. Numerous fault detection approaches have been proposed in literature to diagnose the inter-turn fault from its indications [7]-[11]. The developed fault detection techniques can be mainly classified into two strategies: model-based and model-less methods. The first strategy is based on modeling and estimation analysis applied in PMSM. In faulty operations, the knowledge of how a PMSM behaves can be obtained through appropriate modeling of the PMSM taking into account the turn-to-turn fault. This is a very important step in developing effective detection methods to limit the caused damage and to provide an early fault repair. Normally, PMSM analytical models are derived and validated using Finite Element Methods (FEM). In [11], [12], a modeling and detection method is presented using FEM model for detecting PMSM short-circuit fault. Also a negative sequence analysis is proposed in [15] for PMSM fault detection through a fuzzy logic approach. An alternative fault detection method is based on the analysis of the PMSM magnetic characteristics, where the modeling of faulty impedance has been suggested to detect faults [6]. In addition, estimation techniques have been applied to obtain fault information by means of adaptive PMSM observers [8]. On contrary, the model-less methods can succeed the PMSM fault detection based on the analysis of measured signals,

DOI 10.5013/IJSSST.a.21.02.31

ISSN: 1473-804x online, 1473-8031 print

such as currents, voltages, speed and noise. Depending on the signal analysis, these methods are further classified as time domain methods, frequency domain methods based on Fast Fourier Transform (FFT) and time-frequency domain methods based on wavelet transform [11]. A fault detection algorithm is presented in [10], which is based on the analysis of the PMSM current measurements in time domain. The application of Discrete Fourier Transform (DFT) on the stator currents and the extended Park vector approach has been proposed to detect faults [18]. Detection of the inter-turn short circuit is also proposed in [11] applying Wavelet Packet Analysis (WPA) on PMSM signals. In literature, among the most commonly used detection methods are those based on the machine current signature analysis (MCSA) [9]. However, this analysis may be not appropriate for real time applications due to the complex calculations required for frequency domain transformations.

In this work, a relatively simple technique is proposed to detect phase short-circuit fault in a PMSM based on the faulty dq model through applying the state observer methodology. The fault detection algorithm is focused on a voltage disturbance observer implementation that is able to indicate and quantify the short circuit at specific phase windings. In succeeding this aim, a sliding mode observer (SMO) of stator flux is designed, which allows detecting the stator-winding fault through its *dq* equivalent control inputs. The developed model and the particular sliding mode observer are most of importance in effectively dealing with the problem of fault detection and isolation. Inspecting the estimated disturbance signal allows the evaluation of fault extend and its characteristics as well. A design procedure is described and simulation results are presented to demonstrate the effectiveness of the proposed approach.

Notation:

u_d, u_q = dq axis stator voltages
i_d, i_q = dq axis stator currents
λ_d, λ_q= dq axis stator magnetic fluxes
λ_m= rotor magnetic flux
L_d, L_q = dq axis inductances
r_s = stator resistance
u_γ, u_δ = γδ axis stator voltages
i_γ, i_δ = γδ axis stator currents
λ_γ, λ_δ = γδ axis stator magnetic fluxes
p = number of pole pairs
$\theta=\theta_e$= electrical angular position
$\omega=\omega_e$= electrical angular speed

The rest of this paper is organized as follows: Section II gives the mathematical of faulty PMSM model with an inter-turn short-circuit in phase c. In Section III, a voltage disturbance observer is proposed to estimate the fault effect based on the stator flux calculation. The influence of the shorted turn in phase c is studied in Section IV for different fault-winding fractions σ and different short-circuit current i_f values. Concluding remarks are following in Section V.

II. ANALYSIS OF A SINGLE PHASE FAULT OF PMSM

A. PMSM Model in abc Reference Frame with C-Phase Fault

A turn-to-turn fault is basically an insulation failure between two windings of the same phase. Without loss of generality, it is assumed that the turn fault is located at phase *c*. Particularly, the case of the turn-to-turn fault is demonstrated in Fig. 1 (a). A more detailed diagram of the phase c short-circuit is illustrated in Fig. 1 (b).

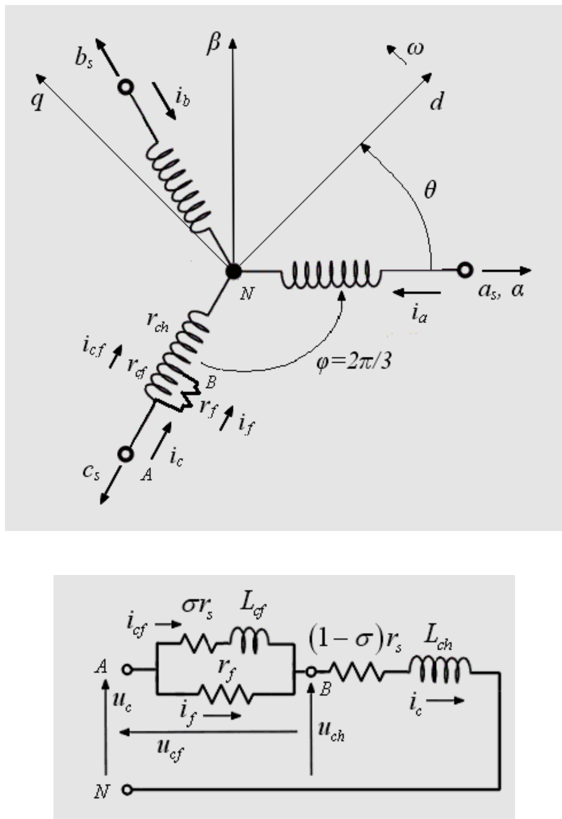

Figure 1. A simplified diagram of the faulty stator winding showing the occurred fault in phase c (upper) and the short-circuit of phase c in more details (lower).

Essentially, the circuit diagram consists of a parallel *R-RL* electric circuit (faulty part, from A to B) and a series *RL* electric circuit (healthy part, from B to N) connected together. The short-circuit fault is occurred at point B, while N is the neutral point. In this simplified diagram, the short circuit is modeled by dividing the *c*-phase windings into two parts namely c_h and c_f representing the healthy and the faulty part of phase *c* respectively. Here it is supposed that the total number of turns of phase *c* is N_c, while the number of short-circuited turns is N_{cf} ($N_{cf} < N_c$). Also, r_{cf} and r_f represent the resistances of faulty part c_f and the sort-circuit respectively, while i_{cf} and i_f are the corresponding currents flowing through the faulty part c_f and the short circuit. Moreover, r_{ch} represents the resistance of healthy part c_h. The fault-winding fraction σ of short-circuited turns to the total number of turns is defined as:

$$\sigma = \frac{N_{cf}}{N_c} = \frac{N_{cf}}{\left(N_{ch} + N_{cf}\right)} < 1 \tag{1}$$

The resistance of healthy part can be calculated as:

$$r_{ch} = \frac{N_{ch}}{N_c} r_s = \frac{N_{ch} - N_f}{N_c} r_s = \left(1-\sigma\right) r_s \tag{2}$$

Accordingly the faulty part resistance of phase c, r_{cf}, is calculated as:

$$r_{cf} = \frac{N_{cf}}{N_c} r_s = \frac{N_{cf}}{N_c} r_s = \sigma r_s \tag{3}$$

Applying Kirchhoff's Current and Voltage Laws (KCL and KVL), the voltage drops of the faulty and healthy part of phase c, u_{cf} and u_{ch}, are given by the following relations:

$$u_{cf} = r_f i_f = \sigma r_s \left(i_c - i_f\right) + \dot{\lambda}_{cf} \tag{4}$$

$$u_{ch} = \left(1-\sigma\right) r_s i_c + \dot{\lambda}_{ch} \tag{5}$$

Adding (4) and (5) by parts, the applied voltage u_c is equal to the sum of the individual voltages u_{cf} and u_{ch}, i.e.

$$\begin{aligned} u_c &= u_{cf} + u_{ch} = r_f i_f + \left(1-\sigma\right) r_s i_c + \dot{\lambda}_{ch} \\ &= \left(1-\sigma\right) r_s i_c + \dot{\lambda}_{ch} + \sigma r_s \left(i_c - i_f\right) + \dot{\lambda}_{cf} \\ &= r_s i_c - \sigma r_s i_c + \left(\dot{\lambda}_{ch} + \dot{\lambda}_{cf}\right) + \sigma r_s i_c - \sigma r_s i_f \\ &= r_s i_c + \left(\dot{\lambda}_{ch} + \dot{\lambda}_{cf}\right) - \sigma r_s i_f = r_s i_c + \dot{\lambda}_c - \sigma r_s i_f \end{aligned} \tag{6}$$

Consequently for a 3-phase PMSM, the voltage equation is written as follows:

$$u_{abc} = r_s i_{abc} + \dot{\lambda}_{abc} - \sigma r_s i_f F_c \tag{7}$$

where

$$u_{abc} = \begin{bmatrix} u_a & u_b & u_c \end{bmatrix}^T = \begin{bmatrix} u_a & u_b & \left(u_{ch} + u_{cf}\right) \end{bmatrix}^T \tag{8}$$

$$i_{abc} = \begin{bmatrix} i_a & i_b & i_c \end{bmatrix}^T = \begin{bmatrix} i_a & i_b & \left[\left(i_c - i_f\right) + i_f\right] \end{bmatrix}^T \tag{9}$$

$$\lambda_{abc} = \begin{bmatrix} \lambda_a & \lambda_b & \lambda_c \end{bmatrix}^T = \begin{bmatrix} \lambda_a & \lambda_b & \left(\lambda_{ch} + \lambda_{cf}\right) \end{bmatrix}^T \tag{10}$$

$$F_c = \begin{bmatrix} 0 & 0 & 1 \end{bmatrix}^T \tag{11}$$

For a symmetrical voltage supply, it is:

$$u_a + u_b + u_c = u_a + u_b + \left(u_{ch} + u_{cf}\right) = 0 \tag{12}$$

Also the stator currents are satisfying the KCL for the phase windings connected in star (see Fig. 1 (a), (b)), i.e.

$$i_a + i_b + i_c = i_a + i_b + \left(i_{cf} + i_f\right) = 0 \tag{13}$$

In addition the stator magnetic flux is defined as:

$$\lambda_{abc} = L_{abcf} i_{abc} + \lambda_m \cos\theta_{abc} \tag{14a}$$

where L_{abcf} is the PMSM inductance matrix in *abc* defined by:

$$L_{abcf} = \begin{bmatrix} L_{aa} & L_{ab} & L_{acf} \\ L_{ba} & L_{bb} & L_{bcf} \\ L_{caf} & L_{cbf} & L_{ccf} \end{bmatrix} \tag{14b}$$

and

$$\cos\theta_{abc} = \begin{bmatrix} \cos\theta & \cos\left(\theta - 2\pi/3\right) & \cos\left(\theta + 2\pi/3\right) \end{bmatrix}^T \tag{15}$$

The subscript (or lower) index *f* in (14b) implies the self and mutual inductances under *inter-turn fault* of phase *c*. Considering the inherent property of saturation, the elements of L_{abc} are supposed to be non-linear functions regarding the stator current vector i_{abc} and short circuit current i_f.

B. PMSM Voltage Model in dq Synchronous Frame with C-Phase Fault

Considering that $u_c = u_{ch} + u_{cf}$, the stator equations can be transformed to the *dq* frame using the synchronous rotating frame transformation matrix K_s defined as follows:

$$K_s = \frac{2}{3} \begin{bmatrix} \cos\theta & \cos\left(\theta - \frac{2\pi}{3}\right) & \cos\left(\theta + \frac{2\pi}{3}\right) \\ -\sin\theta & -\sin\left(\theta - \frac{2\pi}{3}\right) & -\sin\left(\theta + \frac{2\pi}{3}\right) \end{bmatrix} \tag{16}$$

Now multiplying both parts of (7) from the left by K_s, the *dq* components of stator voltage are expressed as:

$$K_s u_{abc} = K_s r_s i_{abc} + K_s \dot{\lambda}_{abc} - K_s \sigma r_s i_f F_c \Leftrightarrow$$

$$K_s u_{abc} = r_s K_s i_{abc} + K_s \frac{d}{dt}\left(K_s^{-1} \lambda_{dq}\right) - \sigma r_s i_f K_s F_c \Leftrightarrow$$

$$u_{dq} = r_s i_{dq} + K_s \left[\frac{d}{dt}\left(K_s^{-1}\right) \lambda_{dq} + K_s^{-1} \dot{\lambda}_{dq}\right] - \sigma r_s i_f K_s F_c \Leftrightarrow$$

$$u_{dq} = r_s i_{dq} + \omega J_s \lambda_{dq} + \dot{\lambda}_{dq}$$
$$-\left(\tfrac{2}{3}\right)\sigma r_s i_f \left[\cos\left(\theta + \tfrac{2\pi}{3}\right) \quad -\sin\left(\theta + \tfrac{2\pi}{3}\right)\right]^T$$
$$= r_s i_{dq} + \omega J_s \lambda_{dq} + \dot{\lambda}_{dq} - d_{dqf} \tag{17}$$

where d_{dqf} represents the voltage disturbance due to the windings fault in phase-c, defined as:

$$d_{dqf} = \sigma r_s i_f K_s F_c = \left(\tfrac{2}{3}\right)\sigma r_s i_f \begin{bmatrix} \cos\left(\theta + \tfrac{2\pi}{3}\right) \\ -\sin\left(\theta + \tfrac{2\pi}{3}\right) \end{bmatrix} \tag{18}$$

and J_s is the 2×2 skew symmetric matrix (J_s= - J_s^T), i.e.

$$J_s = \begin{bmatrix} 0 & -1 \\ 1 & 0 \end{bmatrix} \tag{19}$$

Equation (18) implies that the components of voltage disturbance d_{dqf} are nonlinear functions depending on the short circuit current i_f and rotor angular position θ.

Solving Eq. (17) for $d\lambda_{dq}/dt$, it will be:

$$\dot{\lambda}_{dq} = u_{dq} - r_s i_{dq} - \omega J_s \lambda_{dq} + d_{dqf} \tag{20}$$

C. PMSM Current/Flux Model in dq Synchronous Frame with C-Phase Fault

Multiplying both parts of (14a) from the left by K_s, the *dq* components of stator flux are expressed as:

$$\lambda_{dq} = K_s \lambda_{abc} = K_s L_{abcf} K_s^{-1} K_s i_{abc} + K_s \lambda_m \cos\theta_{abc}$$
$$= L_{dqf} i_{dq} + \lambda_{mdq} = L_{dqf} i_{dq} + \lambda_m \begin{bmatrix} 1 & 0 \end{bmatrix}^T \tag{21}$$

where

$$L_{dqf} = K_s L_{abcf} K_s^{-1} = \begin{bmatrix} L_{ddf} & \Delta L_{dqf} \\ \Delta L_{qdf} & L_{qqf} \end{bmatrix}$$

and

$$\lambda_{mdq} = \lambda_m \begin{bmatrix} 1 & 0 \end{bmatrix}^T$$

Considering *dq* reference frame, the associated inductance matrix λ_{dqf} is non-diagonal in presence of sort-circuit fault. Normally, the mutual inductances ΔL_{dqf} and ΔL_{qdf} are non zero elements in L_{dqf} inductance matrix.

III. FLUX OBSERVER DESIGN UNDER A SINGLE PHASE FAULT

A. Design of Stator Flux Observer in dq Reference Frame

The design procedure of SMO consists of two main steps: hyperplane or manifold design and control law design based on the sliding mode existence conditions. For sliding manifold definition, the stator flux errors are used as sliding surfaces, i.e. $s_d = \lambda_d - \hat{\lambda}_d = \bar{\lambda}_d$ and $s_q = \lambda_q - \hat{\lambda}_q = \bar{\lambda}_q$, where the symbol ^ implies in general estimated values of PMSM variables. The proposed flux SMO is defined by:

$$\dot{\hat{\lambda}}_{dq} = u_{dq} - \hat{r}_s i_{dq} - \omega J_s \hat{\lambda}_{dq} + k_{dq} sign\bar{\lambda}_{dq} \tag{22}$$

After subtracting (22) from (19), the flux observer dynamics is written as:

$$\dot{\bar{\lambda}}_{dq} = \dot{s}_{dq} = -\bar{r}_s i_{dq} - \omega J_s \bar{\lambda}_{dq} + d_{dqf} - k_{dq} sign\bar{\lambda}_{dq} \tag{23}$$

or more analytically:

$$\dot{\bar{\lambda}}_d = -\bar{r}_s i_d + \omega \bar{\lambda}_q + d_{df} - k_d sign\bar{\lambda}_d \tag{24a}$$
$$\dot{\bar{\lambda}}_q = -\bar{r}_s i_q - \omega \bar{\lambda}_d + d_{qf} - k_q sign\bar{\lambda}_q \tag{24b}$$

Here k_d>0, k_q>0 are the SMO gains. The stability of the above system of (23) (or (24a) and (24b)) is considered in sense of Lyapunov and it is closely related to the choice of k_d and k_q. Let the positive definite function V_λ be a Lyapunov function candidate (LFC), defined as follows:

$$V_\lambda = \frac{1}{2}\left[\left(\bar{\lambda}_d\right)^2 + \left(\bar{\lambda}_q\right)^2 + \frac{1}{k_r}\left(\bar{r}_s\right)^2\right] \geq 0 \tag{25}$$

where $k_r>0$ is the gain of the stator resistance observer.

Differentiating both sides of (25) with respect to time, the dV_λ/dt may be written as:

$$\dot{V}_\lambda = \bar{\lambda}_d \dot{\bar{\lambda}}_d + \bar{\lambda}_q \dot{\bar{\lambda}}_q + \frac{1}{k_r}\bar{r}_s \dot{\bar{r}}_s$$
$$= \bar{\lambda}_d \left(-\bar{r}_s i_d + \omega \bar{\lambda}_q + d_{df} - k_d sign\bar{\lambda}_d\right)$$
$$+ \bar{\lambda}_q \left(-\bar{r}_s i_q - \omega \bar{\lambda}_d + d_{qf} - k_q sign\bar{\lambda}_q\right) + \frac{1}{k_r}\bar{r}_s \dot{\bar{r}}_s$$
$$= -k_d \left|\bar{\lambda}_d\right| - \bar{r}_s i_d \bar{\lambda}_d + \omega \bar{\lambda}_q \bar{\lambda}_d + d_{df} \bar{\lambda}_d$$

$$-k_q\left|\bar{\lambda}_q\right|-\bar{r}_s i_q\bar{\lambda}_q-\omega\bar{\lambda}_d\bar{\lambda}_q+d_{qf}\bar{\lambda}_q+\frac{1}{k_r}\bar{r}_s\dot{\bar{r}}_s$$
$$=-k_d\left|\bar{\lambda}_d\right|-k_q\left|\bar{\lambda}_q\right|+\frac{1}{k_r}\bar{r}_s\left[\dot{\bar{r}}_s-k_r\left(i_d\bar{\lambda}_d+i_q\bar{\lambda}_q\right)\right]$$
$$+\bar{\lambda}_d d_{df}+\bar{\lambda}_q d_{qf}\leq 0 \tag{26}$$

The observer asymptotic stability is ensured, if the derivative of LFC is negative definite, i.e. $dV_\lambda/dt<0$. Consequently, this is valid, if the following conditions are satisfied:

$$k_d>\left|-\bar{r}_s i_d+\omega\bar{\lambda}_q\right|+\left|d_{df}\right|>\left|d_{df}\right| \tag{27a}$$
$$k_q>\left|-\bar{r}_s i_q\bar{\lambda}_q-\omega\bar{\lambda}_d\right|+\left|d_{qf}\right|>\left|d_{qf}\right| \tag{27b}$$
$$\dot{\bar{r}}_s-k_r\left(i_d\bar{\lambda}_d+i_q\bar{\lambda}_q\right)=0 \tag{27c}$$

B. Voltage Disturbance Estimation Based on Equivalent Control Method

Assuming that the Stator flux observer in (23) and stator resistance estimator in (27c) converge considerably fast, the sliding manifold is reached ($s_{dq}=0$) after finite time t_n. Therefore the state trajectories satisfy the initial system equation with the control inputs replaced by their equivalent ones after setting $ds_{dq}/dt=0$ in (24a), and (24b), i.e.

$$d_{df}-\left(k_d\operatorname{sgn}\bar{\lambda}_{df}\right)_{eq}=0\Leftrightarrow d_{df}=\left(k_d\operatorname{sgn}\bar{\lambda}_{df}\right)_{eq} \tag{28a}$$
$$d_{qf}-\left(k_q\operatorname{sgn}\bar{\lambda}_q\right)_{eq}=0\Leftrightarrow d_{qf}=\left(k_q\operatorname{sgn}\bar{\lambda}_q\right)_{eq} \tag{28b}$$

Here the terms $(.)_{eq}$ represent the equivalent inputs. Information for the voltage disturbance could be obtained directly by means of low pass filtering (LPF) the control input signals of SMO.

IV. SIMULATION RESULTS

The presented method was tested and verified on a PMSM with parameters listed in Table I.

TABLE I. PARAMETERS OF SM WITH ROTOR FIELD WINDING

Symbol	Quantity	Expressed in SI
S	electric power	5.5 kVA
$cos\varphi$	electric power coefficient	0.8
V_{l-l}	line to line voltage	380 V
r_s	stator resistance	2.5 Ω
L_{md}	d-axis inductance	0.360 H
L_d	d-axis inductance	0.400 H
L_q	q-axis inductance	0.210 H
λ_m	permanent magnets flux	0.5 Vs
J	moment of inertia	0.089 kgm^2
p	magnetic pole pairs	1
ω_m	mechanical angular speed	3000 rpm

Simulations tests are curried out using the Simulink/Matlab application. An antiwindup controller (AWC) has been embedded into the speed controller to avoid windup phenomena by means of a saturation element. Here the AWC is regulated to limit the stator current between –8A and 8A. Also the switching frequency of the voltage source inverter (VSI) is 5kHz with a DC voltage equal to 400V while operating in SVPWM (Space Vector Pulse Width Modulation) mode. In the simulation, it is assumed that the stator resistance changes between 1.0 and 1.2 of its nominal value. In next paragraphs, the estimation of stator flux and voltage disturbance is evaluated for low to middle speed region with reference speed at 5 Hz (300rpm) and 10Hz (600rpm).

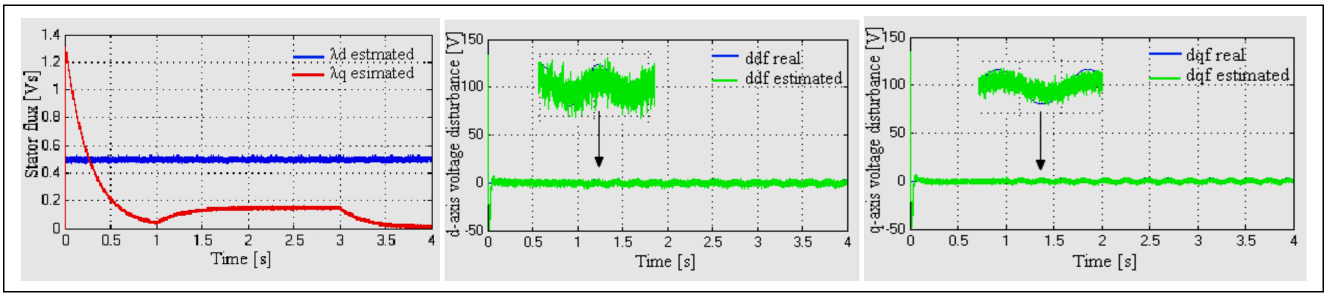

Figure 2. Estimated stator flux in dq reference frame (left), voltage disturbances in d-axis (middle) and q-axis (right). The speed was changed from 0 to 10π rad/s stepwise, while an external torque of 1.0Nm is applied for 2s.

A. Evaluation of Stator Fault Observer at 10π rad/s (or 300rpm)

Here it is supposed that the windings ratio σ is equal τo 0.5 and the sort-circuit current i_f is 4A. In simulation results presented, initially the speed reference is changed stepwise from 0 of 10ð rad/s. Afterwards, an external torque disturbance of 1.0Nm was applied at t_1=1s and removed at t_3=3s. The real and estimated/observed values of d_{dqf} are demonstrated in Fig. 2 (middle and right part) respectively, while Fig. 2 (left part) shows the estimated stator flux. The error between the real and the observed stator flux is about

0.01 Vs with a maximum of 0.015 Vs during transition from zero to positive external torque. It is observed that voltage disturbances, d_{df} and d_{qf}, fluctuate between –4.0V to 4.0V. Estimated stator flux and voltage disturbances in d- and q-axis show the efficiency and robustness of the estimation scheme, since both observed PMSM variables are estimated with very good accuracy.

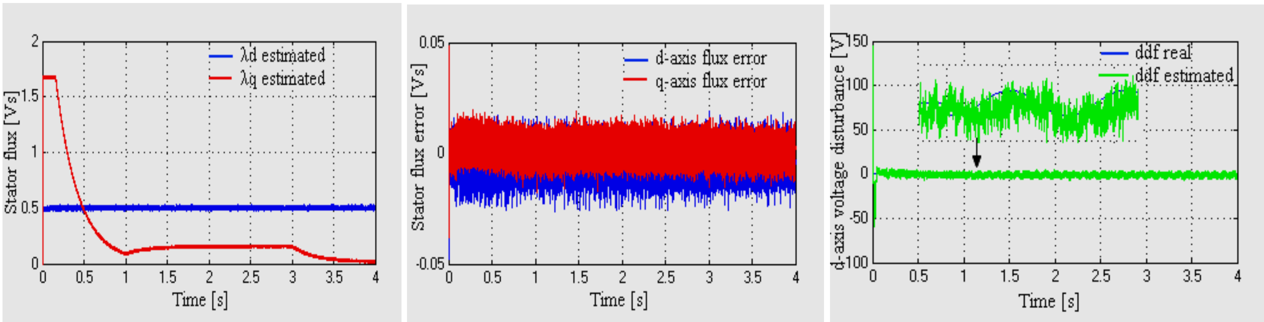

Figure 3. Estimated stator flux in dq reference frame (left), stator flux error (middle) and voltage disturbance in d-axis (right). The speed was changed from 0 to 20π rad/s stepwise, while an external torque of 1.0Nm is applied for 2s.

B. Evaluation of Stator Fault Observer at 20π rad/s (or 600rpm).

In this case the windings ratio σ is set equal τo 0.2 and the sort-circuit current i_f is set equal to 5A. Initially the speed reference is changed stepwise from 0 of 20ð rad/s. Also the same external torque disturbance of 1.0Nm was applied at t_1=1s and removed at t_3=3s. The real and estimated/observed values of stator d_{df} are demonstrated in Fig. 3 (lower part) respectively, while Fig. 3 (upper part) shows the estimated stator flux and its error. The error between the real and the observed stator flux is about 0.02 Vs with a maximum of 0.025 Vs during transition states. It is observed that voltage disturbances, d_{df} and d_{qf}, fluctuate between –2.25V to 2.25V. Decreasing chattering phenomenon in SMO, the observer response could be further improved.

V. CONCLUSION

In this work, a dq PMSM mathematical model was presented under of one single-phase short-circuit fault. Based on the detailed dq model, a sliding mode observer has been developed for estimation of voltage disturbances that allows the detection of inter-turn faults. In the designed sliding mode observer, the voltage disturbance information was extracted from the derived equivalent control signals. Based on the PMSM model analysis, it is showed that the stator flux observer established is robust and computationally efficient providing accurate disturbance estimation. The proposed model-observer scheme provides an effective tool for evaluating the PMSM behavior under several malfunctioning modes due to inter-turn fault. Simulations results validated that the fault influence on the PMSM operation could be detected and recognized with relatively high accuracy providing very important information about machine operating conditions.

REFERENCES

[1] P. C. Krause, O. Wasynczuk, and S. D. Sudhoff, “Analysis of electric machinery and drive systems”, 2nd ed., Wiley-IEEE, New York, 2002.

[2] R. Krishan, “Electric motor drives: Modelling, analysis and control,” Prentice Hall Company, New Jersey, 2001.

[3] J. A. Rosero, L. Romeral, J. A. Ortega, and E. Rosero, “Short-Circuit Detection by Means of Empirical Mode Decomposition and Wigner-Ville Distribution for PMSM Running Under Dynamic Condition,” IEEE Trans. Ind. Electron., vol. 56, no. 11, pp. 4534–4547, Nov. 2009.

[4] A. H. Bonnett and G. C. Soukup, “Cause and analysis of stator and rotor failures in three-phase squirrel-cage induction motors,” IEEE Trans. Ind. Appl., vol. 28, no. 4, pp. 921–937, 1992.

[5] A. Sarikhani and O. A. Mohammed, “Inter-turn fault modeling of a variable speed pm wind generator using physics-based approach,” in Electric Machines Drives Conference (IEMDC), 2011 IEEE International, 2011, pp. 636–641.

[6] N. Leboeuf, T. Boileau, B. Nahid-Mobarakeh, N. Takorabet, F. Meibody-Tabar, and G. Clerc, “Inductance Calculations in Permanent-Magnet Motors Under Fault Conditions,” IEEE Trans. Magn., vol. 48, no. 10, pp. 2605–2616, Oct. 2012.

[7] Z. Sun, J. Wang, D. Howe, and G. Jewell, “Analytical Prediction of the Short-Circuit Current in Fault-Tolerant Permanent-Magnet Machines,” IEEE Trans. Ind. Electron., vol. 55, no. 12, pp. 4210 –4217, Dec. 2008.

[8] A. Sarikhani and O. A. Mohammed, “Inter-Turn Fault Detection in PM Synchronous Machines by Physics-Based Back Electromotive Force Estimation,” IEEE Trans. Ind. Electron., vol. 60, no. 8, pp. 3472–3484, Aug. 2013.

[9] B.-M. Ebrahimi and J. Faiz, “Feature Extraction for Short-Circuit Fault Detection in Permanent-Magnet Synchronous Motors Using Stator-Current Monitoring,” IEEE Trans. Power Electron., vol. 25, no. 10, pp. 2673–2682, 2010.

[10] Manuel A. Mazzoletti, Guillermo R. Bossio, Cristian H. De Angelo, and Diego R. Espinoza-Trejo, “A Model-Based Strategy for Interturn

DOI 10.5013/IJSSST.a.21.02.31 ISSN: 1473-804x online, 1473-8031 print

Short-Circuit Fault Diagnosis in PMSM," IEEE Trans. Ind. Appl., vol. 64, no. 9, pp. 7218-7228, Sep. 2017.

[11] O. A. Mohammed, Z. Liu, S. Liu, and N. Y. Abed, "Internal Short Circuit Fault Diagnosis for PM Machines Using FE-Based Phase Variable Model and Wavelets Analysis," IEEE Trans. Magn., vol. 43, no. 4, pp. 1729–1732, Apr. 2007.

[12] Y.-S. Lee, K.-T. Kim, and J. Hur, "Finite-Element Analysis of the Demagnetization of IPM-Type BLDC Motor With Stator Turn Fault," IEEE Trans. Magn., vol. 50, no. 2, pp. 889–892, Feb. 2014.

[13] K.-T. Kim, J. Park, B. Kim, and J. Hur, "Comparison of the fault characteristics of IPM-type and SPM-type BLDC motors under Inter-Turn Faults conditions using Winding Function Theory," in 2012 IEEE Energy Conversion Congress and Exposition (ECCE), 2012, pp. 1262 –1269.

[14] M. Riera Guasp, J. A. Antonino-Daviu, and G. A. Capolino, "Advances in Electrical Machine, Power Electronic, and Drive Condition Monitoring and Fault Detection: State of the Art," IEEE Trans. Ind. Electron., vol. 62, no. 3, pp. 1746–1759, Mar. 2015.

[15] J. Quiroga, Li Liu, and D. A. Cartes, "Fuzzy Logic Based Fault Detection of PMSM Stator Winding Short Underload Fluctuation Using Negative Sequencr," Proceeding in 2008 American Control Conference (ACC 2008), pp. 4262–4267, 11-13 June 2008, Seattle, WA, USA.

[16] Y. Lee and T. G. Habetler, "A Phase Variable Simulation Model for Interior PM Synchronous Motor Drives with Stator Turn Faults," Proceedings of Power Electronics and Motion Control Conference, (EPE-PEMC 2006), 2006, pp. 1074 –1079.

[17] Bhaskar Sen, and Jiabin Wang, "Stator Inter-Turn Fault Detection in Permanent Magnet Machines Using PWM Ripple Current Measurement," IEEE Trans. Ind. Electr., vol. 63, no. 5, pp. 3148 - 3157, May 2016.

[18] Y. Lee, "A Stator Turn Fault Detection Method and a Fault-Tolerant Operating Strategy for Interior PM Synchronous Motor Drives in Safety-Critical Applications," PhD Thesis, Georgia Institute of Technology, 2007.

[19] S. Nadarajan, S. K. Panda, B. Bhangu, and A. K. Gupta, "Hybrid Model for Wound-Rotor Synchronous Generator to Detect and Diagnose Turn-to-Turn Short-Circuit Fault in Stator Windings," IEEE Trans. Ind. Electron., vol. 62, no. 3, pp. 1888–1900, Mar. 2015.

[20] X. Chen, J. Wang, B. Sen, P. Lazari, and T. Sun, "A High-Fidelity, Computationally Efficient Model for Interior Permanent Magnet Machines Considering the Magnetic Saturation, Spatial Harmonics and Iron Loss Effect," IEEE Trans. Ind. Electron., vol. 62, no. 7, pp. 4044–4055, Jul. 2015.

[21] K.-T. Kim, J.-K. Park, J. Hur, and B.-W. Kim, "Comparison of the Fault Characteristics of IPM-Type and SPM-Type BLDC Motors Under Inter-Turn Fault Conditions Using Winding Function Theory," IEEE Trans. Ind. Appl., vol. 50, no. 2, pp. 986–994, Mar. 2014.

[22] K.-T. Kim, J. Hur, B. Kim, and G.-H. Kang, "Circulating current calculation using fault modeling of IPM type BLDC motor of inter-turn fault," in 2011 International Conference on Electrical Machines and Systems (ICEMS), 2011, pp. 1 –5.

[23] M. Boesing, M. Niessen, T. Lange, and R. De Doncker, "Modeling spatial harmonics and switching frequencies in PM synchronous machines and their electromagnetic forces," in 2012 XXth International Conference on Electrical Machines (ICEM), 2012, pp. 3001–3007.

[24] M. Boesing, M. Niessen, T. Lange, and R. De Doncker, "Modeling spatial harmonics and switching frequencies in PM synchronous machines and their electromagnetic forces," in 2012 XXth International Conference on Electrical Machines (ICEM), 2012, pp. 3001–3007.

[25] Park, J.-K.; Jeong, C.-L.; Lee, S.-T.; Hur, J. Early detection technique for stator winding inter-turn fault in BLDC motor using input impedance. IEEE Trans. Ind. Appl. 2015, 51, 240–247.

[26] T. G. Habetler and Y. Lee, "Current-based condition monitoring and fault tolerant operation for electric machines in automotive applications," in International Conference on Electrical Machines and Systems, 2007. ICEMS, 2007, pp. 2011 –2016.

[27] Lee, S.-T.; Hur, J. Detection Technique for Stator Inter-Turn Faults in BLDC Motors Based on Third-Harmonic Components of Line Currents. IEEE Trans. Ind. Appl. 2017, 53, 143–150.

[28] Haddad, R.Z.; Strangas, E.G. Detection of static eccentricity and turn-to-turn short circuit faults in permanent magnet synchronous AC machines. In Proceedings of the 2015 IEEE 10th International Symposium on Diagnostics for Electrical Machines, Power Electronics and Drives (SDEMPED), Guarda, Portugal, 1–4 September 2014; pp. 277–283.